JACS
JOURNAL OF THE AMERICAN CHEMICAL SOCIETY
Article
pubs.acs.org/JACS

Oligonaphthofurans: Fan-Shaped and Three-Dimensional π-Compounds

Kentaro Nakanishi,[†] Daisuke Fukatsu,[‡] Kazuto Takaishi,[§,∥] Taiki Tsuji,[†] Keita Uenaka,[†] Kouji Kuramochi,[†] Takeo Kawabata,[‡] and Kazunori Tsubaki*[,†]

[†]Graduate School of Life and Environmental Sciences, Kyoto Prefectural University, Shimogamo, Sakyo-ku, Kyoto 606-8522, Japan
[‡]Institute for Chemical Research, Kyoto University, Uji, Kyoto 611-0011, Japan
[§]Faculty of Science and Technology, Seikei University, Musashino, Tokyo 180-8633, Japan
[∥]RIKEN, Wako, Saitama 351-0198, Japan

Supporting Information

ABSTRACT: Using a bottom-up method, we prepared a series of oligonaphthofurans composed of alternating naphthalene rings and furan rings. The largest compound (compound **25**) contained 8 naphthalene units and 7 furan units. DFT calculations revealed that these compounds were fan-shaped molecules and each naphthalene ring was oriented in an alternate mountain-valley fold conformation because of steric repulsion by the hydrogens at the *peri*-positions. We investigated the optical properties that derived from their fan-shaped and mountain-valley sequences. As the number of aromatic rings of the oligonaphthofurans increased, the peaks of the longest wavelength absorptions in the UV−vis spectra (HOMO−LUMO energy gap) of these compounds steadily red-shifted, although the shapes of spectra were not sustained because of the decreasing molar absorption coefficients (ε's) of their λ_{max}. We compared our results with those reported for other types of oligoaromatic compounds such as acenes **1**, ethene-bridged *p*-phenylenes **2**, rylenes **3**, oligofurans **4**, and oligonaphthalenes **5**. The slopes of the plots between the transition energies (HOMO−LUMO energy gap) of the oligoaromatic compounds and the reciprocal of the number of aromatic rings indicated that the efficiency of π conjugation of the oligonaphthofurans was comparable with that of linear and rigid acenes and rylenes. The higher-order compounds **22** and **25** aggregated even under high dilution conditions (~10^{-6} M).

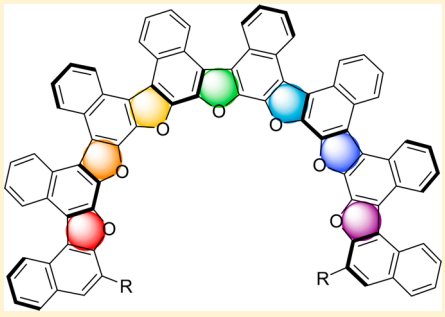

INTRODUCTION

Oligoaromatic compounds, which are composed of connecting or conjugated aromatic rings, have attracted much attention because of the beauty of their structures and their useful functions such as in innovative electronic and near-infrared materials.[1] These oligoaromatic compounds are classified by their fragmental aromatic rings (thus benzenoids, non-benzenoids including hydrocarbons, and hetero aromatic including compounds) and the direction of their π system extension (thus two-dimensional or three-dimensional compounds). Representative aromatic compounds are shown in Figure 1.

As for two-dimensional benzenoid polycyclic aromatic hydrocarbons (BPAHs), linearly fused benzene oligomers (acenes **1**; up to 9 fused benzene rings = nonacene)[2] and ethene-bridged *p*-phenylene oligomers **2** (up to 13 fused benzene rings)[3] were reported by Anthony and Liu, respectively. Müllen reported *peri*-fused naphthalene oligomers (rylenes **3**; up to a 6mer) and introduced a hexarylene derivative with an absorption maximum around 950 nm.[4] Recently, Peña et al. introduced a clover-shaped *cata*-condensed PAH (cloverphene with up to 16 fused benzene rings).[5] Furthermore, as examples of polycyclic hydrocarbons with five-membered rings (cyclopentadienes), ladder-type oligonaphthalenes (up to 5 fused naphthalene rings and 4 cyclopentadienes),[6] and indenofluorenes,[7] which have a singlet diradical character, have also been reported. Moreover, the unique properties of the 3D framework of aromatic compounds such as fullerenes and their segmental corannulene[8] and sumanene,[9] carbon nanotubes and their segmental cycloparaphenylenes[10] and related carbon nanocages,[11a,b] have also been demonstrated.[12] With respect to typical examples of oligoaromatic compounds with hetero aromatic rings, oligothiophenes,[13] oligofurans,[14] and three-dimensional helicene types containing thiophenes and furans have also been synthesized, and their functions have been reported.

With this background, our research initially focused on chiral helical oligonaphthalenes **5** where each naphthalene ring is connected at the 1,4-positions. We prepared compounds up to all-(*S*)-32mers via a bottom-up procedure.[15,16] These oligonaphthalenes **5** exhibit peculiar functions (i.e., hierarchical energy transfer through the axes and CD properties because of their rigid rod-shaped structures).[17] However, the nearly

Received: March 11, 2014
Published: April 17, 2014

   dx.doi.org/10.1021/ja502209w | J. Am. Chem. Soc. 2014, 136, 7101−7109

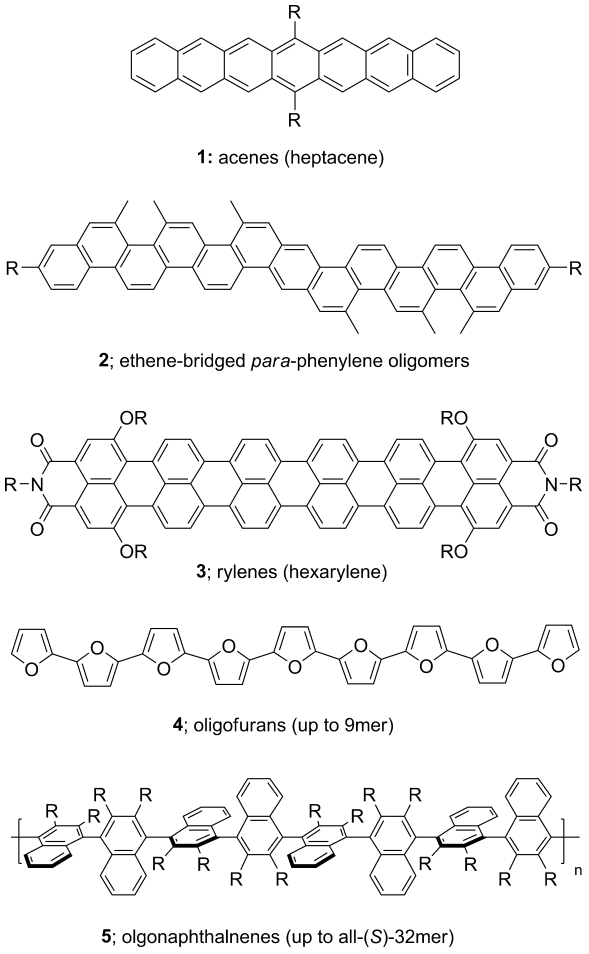

Figure 1. Related oligoaromatic compounds.

orthogonal arrangement causes the extensive π-conjugation between the adjacent naphthalene rings to be ineffective.

More recently, we systematically investigated the characteristics of spreading the π-system and controlling the dihedral angles by incorporating an axis in the ring structure. We have already reported an oligonaphthodioxepine (fused seven-membered ring) in which the dihedral angle of the adjacent naphthalene unit is controlled at ca. 48°, and its fluorescence properties in the solid state were investigated.[18]

Herein, we report that the incorporation of an axis into a five-membered furan ring results in fan-shaped oligonaphthofurans in which the dihedral angles are narrowed (ca. 20°).[19] Revealing the chemical and physical properties of these 3D π-systems and determining the number of furans and naphthalenes that can be incorporated are of interest.[20] Figure 2 shows that these compounds have unique fan-shaped structures composed of alternating furan and naphthalene rings. Additionally, the 3D π-systems are derived from repulsion between the hydrogens at the *peri*-positions.

To the best of our knowledge, previous studies have focused on the dihedral angle; Osuka et al. have evolved a *meso-meso*-linked porphyrin array in which each porphyrin is connected at the *meso*-position with a 90° dihedral angle[21] into a porphyrin tape in which each porphyrin ring is fused in a planar fashion.[22]

RESULTS AND DISCUSSION

Synthesis of the Naphthofuran 3mer. To construct a series of oligonaphthofurans using the bottom-up method, we

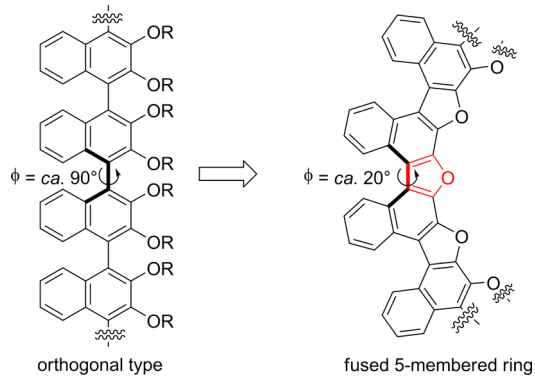

Figure 2. From orthogonal oligonaphthalenes to fan-shaped oligonaphthofurans.

selected naphthofuran 2mer **6** as a suitable synthon. Compound **6** was synthesized by the dehydration of binaphthol under acidic conditions (CH_3SO_3H, toluene reflux).[23] Scheme 1 shows the synthetic route for the naphthofuran 3mer **10** from

Scheme 1. Synthesis of Naphthofuran 3mer 10[a]

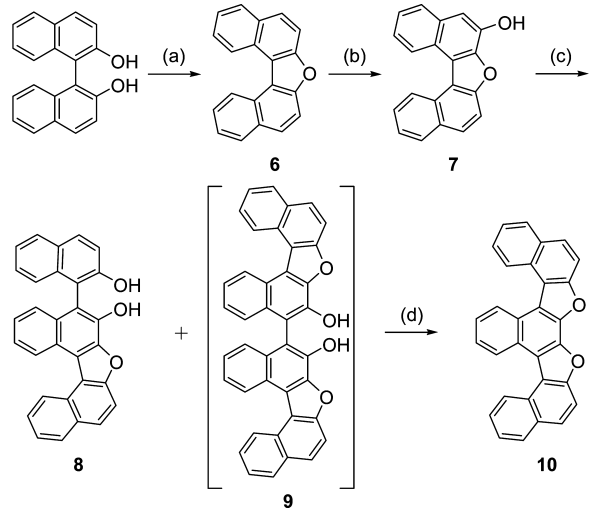

[a]Reagents and conditions: (a) CH_3SO_3H, 94%; (b) (1) *n*-BuLi, (2) $B(OMe)_3$, (3) H_2O_2, 92% for 3 steps; (c) 2-naphthol (9 equiv), $CuCl_2$, *n*-Pr_2NH, 37%; (d) CH_3SO_3H, 76%.

6. Using a modification of a reported procedure,[24] the initial naphthofuran 2mer **6** was *ortho*-lithiated by *n*-BuLi and allowed to successively react with $B(OMe)_3$ and 30% aqueous H_2O_2 to afford compound **7** in 92% yield over three steps. Heterocoupling between compound **7** and an excessive amount of 2-naphthol (9 equiv) occurred in the presence of $CuCl_2$ (20 equiv) as an oxidant together with *n*-Pr_2NH to give the desired (2+1)-3mer **8** (37% yield based on compound **7**) and the homocoupling adduct (2+2)-4mer **9** (60% yield based on **7**) with a large amount of binaphthol.[25] After the isolation and purification of (2+1)-3mer **8** by column chromatography, the furan ring was constructed by a dehydration of the two hydroxy groups of **8** in the presence of CH_3SO_3H (2 equiv) under toluene reflux conditions to give naphthofuran 3mer **10** in 76% yield.

Synthesis of the Naphthofuran 4mer. Compound **7** was homocoupled using $CuCl_2$ and *n*-Pr_2NH to give the desired (2+2)-4mer **9** in 94% yield (Scheme 2).[26] The attempted

dx.doi.org/10.1021/ja502209w | *J. Am. Chem. Soc.* 2014, 136, 7101−7109

Scheme 2. Synthesis of Naphthofuran 4mers 14 and 15 and (2+2)-4mer 16[a]

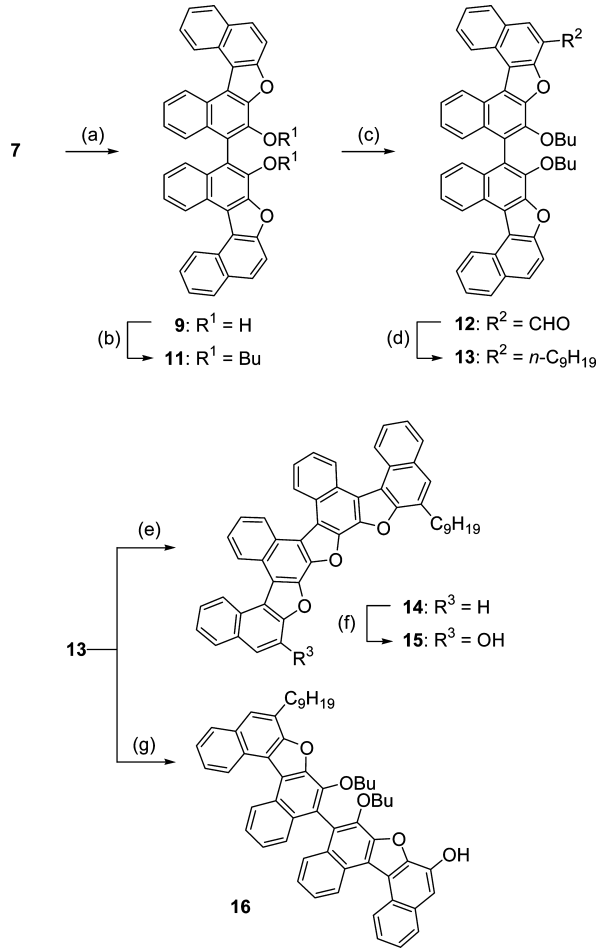

[a]Reagents and conditions: (a) $CuCl_2$, *n*-Pr_2NH, 94%; (b) *n*-BuBr, K_2CO_3, 83%; (c) *n*-BuLi, DMF, 56%; (d) (1) $Ph_3P{=}CHC_7H_{15}$, (2) H_2, Pd/C, 89% for 2 steps; (e) CF_3SO_3H, 78%; (f) (1) *n*-BuLi, (2) $B(OMe)_3$, (3) H_2O_2, 92% for 3 steps; (g) (1) *n*-BuLi, (2) $B(OMe)_3$, (3) H_2O_2, 92% for 3 steps.

dehydration of (2+2)-4mer **9** in the presence of CH_3SO_3H gave a residue, which was inferred to be the naphthofuran 4mer. However, because of the residue's very low solubility in all solvents, it was impossible to determine its structure and use it as an intermediate for further higher-order oligonaphthofurans. To enhance its solubility, we planned to introduce alkyl chains onto the *ortho*-position of (2+2)-4mer **9**. Thus, two *n*-Bu groups were tentatively introduced to the central hydroxy groups of **9**. These groups served both as a protecting group and a modulator of solubility to give **11** in 83% yield. Compound **11** was *ortho*-monolithiated by *n*-BuLi (1.2 equiv) and trapped by DMF to convert it to the formyl derivative **12** and to recover **11** in respective yields of 56% and 18%. A Wittig reaction was performed using compound **11** and *n*-octyltriphenylphosphonium bromide, and then the double bond was hydrogenated by H_2 under Pd/C conditions to introduce the *n*-nonyl side chain as a new solubility modulator, affording compound **13** in 89% yield over two steps. Compound **13** was treated with CF_3SO_3H (2 equiv) in *o*-xylene at 130 °C for 24 h to remove the two butyl groups. The successive formation of the furan ring via the dehydration of the hydroxy groups afforded the corresponding naphthofuran 4mer **14** in 78% yield. The important intermediate **15**, which possessed a scaffolding hydroxy group for further higher-order oligonaphthofurans, was constructed through *ortho*-lithiation, the introduction of dimethoxyboran, and oxidation using 30% aqueous H_2O_2 to give the product in 92% yield over three steps from compound **14**. The same sequence was applied to **13** to afford compound **16**, which was another important intermediate for further higher-order oligonaphthofurans, and it was obtained in 92% overall yield.

In contrast, starting from a binaphthol possessing two *n*-octyl chains on the 6,6′ -positions was not fruitful. Because of steric repulsion between the alkyl side chains of the adjacent naphthalenes, no furan ring formation upon the second conversion from **17** to **18** occurred (Scheme 3). Thus,

Scheme 3. Attempted Furan Ring Formation from Compound 17[a]

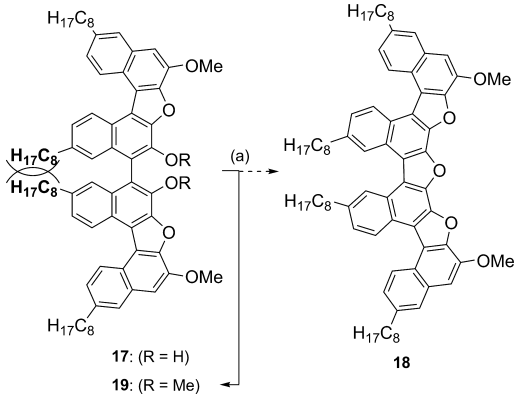

[a]Reagents and conditions: (a) (1) CF_3SO_3H, (2) MeI, K_2CO_3, 50% for **19**, not obtained for **18**.

compound **17** was subjected to the same conditions as the transformation from **13** to **14**. Because the methoxy groups on the top and bottom naphthalenes of **17** were partially removed under these reaction conditions, the residue was successively treated with MeI and K_2CO_3. However, the desired compound **18** was not obtained at all, and methylated **19** was obtained in 50% yield instead (for the investigated synthetic route, see the Supporting Information).

Synthesis of the Naphthofuran 6mer. Upon repeating the procedure, (4+2)-6mer **20** was derived from the heterocoupling of **7** (9 equiv) and naphthofuran 4mer **15** (1 equiv) in 29% yield (Scheme 4). For this reaction, the homocoupling of each component occurred instead of the desired heterocoupling. In contrast, for the coupling between (2+2)-4mer **16** and 2mer **7** under the same reaction conditions, the yield of the desired (2+2+2)-6mer **21**, which was obtained as a diastereomeric mixture with respect to the two axes bonds, improved significantly to 59%. The naphthofuran 6mer **22** from both **20** and **21** was obtained in moderate yields. Thus, treating **20** with *p*-TsOH (20 equiv) in refluxing *o*-xylene for 24 h gave the desired naphthofuran 6mer **22** in 24% yield. The treatment of (2+2+2)-6mer **21** with CF_3SO_3H (5 equiv) in *o*-xylene at 160 °C (sealed tube conditions) for 3 days led to the removal of the butyl side chains, and two furan rings formed to afford naphthofuran 6mer **22** in 27% yield.

Synthesis of Naphthofuran 8mer. We then tried to synthesize naphthofuran 8mer **25** using the following two approaches (Scheme 5). The first approach was through (4+4)-

dx.doi.org/10.1021/ja502209w | J. Am. Chem. Soc. 2014, 136, 7101−7109

Scheme 4. Synthesis of Naphthofuran 6mer 22[a]

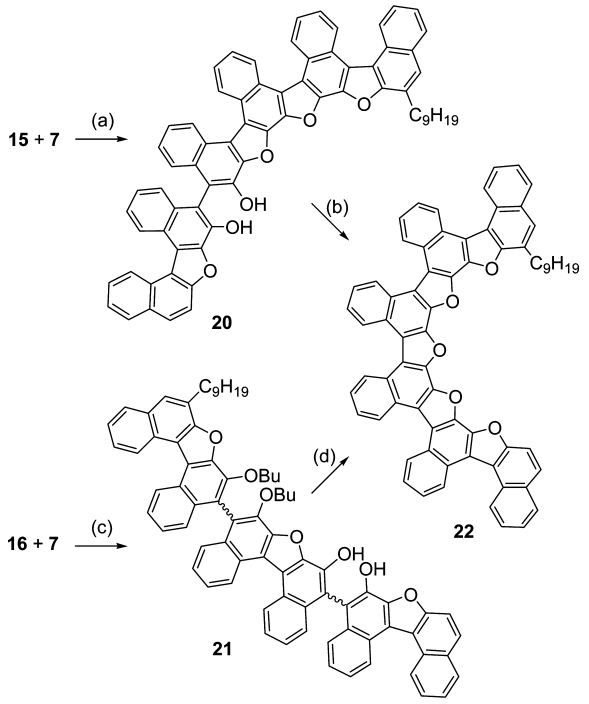

[a]Reagents and conditions: (a) $CuCl_2$, *n*-Pr_2NH, 29%; (b) *p*-TsOH, 24%; (c) $CuCl_2$, *n*-Pr_2NH, 59%; (d) CF_3SO_3H, 27%.

Scheme 5. Synthesis of Naphthofuran 8mer 25[a]

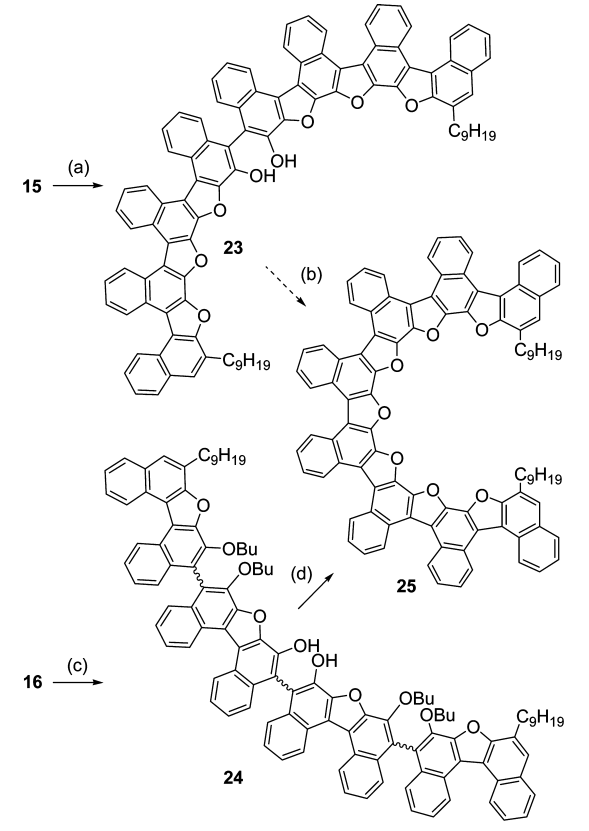

[a]Reagents and conditions: (a) $CuCl_2$, *n*-Pr_2NH, 68%; (b) CF_3SO_3H, not obtained; (c) $CuCl_2$, *n*-Pr_2NH, 84%; (d) CF_3SO_3H, 16%.

8mer **23**, and the other was through (2+2+2+2)-8mer **24**. Precursors **23** and **24** were derived from the corresponding monomers **15** and **16** using optimized oxidative coupling conditions ($CuCl_2$ and *n*-Pr_2NH) in 68% and 84% yields, respectively. The construction of a central furan ring from (4+4)-8mer **23** seemed to be the most direct and reasonable way to achieve our goal; however, this strategy came to nothing. Even though (4+4)-8mer **23** was treated with CF_3SO_3H (10 equiv) in *o*-xylene at 160 °C for 30 days (sealed tube), no desired product was obtained. A DFT calculation at the B3LYP/6-31G(d,p) level indicated that the (4+4)-8mer is about 3.4 kcal/mol more stable than the (7+1)-8mer, and therefore, the drastic increase in strain energy during the final step may prevent cyclization (see Supporting Information).[27]

In contrast, (2+2+2+2)-8mer **24** was treated under the same conditions, and the reaction was monitored by TLC. Many reactions (deregulated removal of the four butyl chains, three random closings of the furan rings, and the disorderly epimerization of the three connecting axes) were initially observed but gradually converged into a single yellow fluorescent spot. The desired naphthofuran 8mer **25** was finally isolated in 16% yield. The structure of naphthofuran 8mer **25** was confirmed via changes in its NMR spectra (although the signals of 8mer **25** were extremely broad because of self-aggregation, the signals from the butyl side chains and phenolic hydroxy protons clearly disappeared), and a good correlation was obtained between the theoretical and experimental values for the isotopic distribution in the high-resolution mass spectrum of **25**.

With respect to the conformation of the naphthofuran 8mer, DFT calculations at the B3LYP/6-31G(d,p) level after a zero-point energy correlation revealed that the alternating mountain-valley fold conformation was about 11 kcal/mol more stable than the homochiral screw-shaped conformation (Figure 3). The reported X-ray structure of the thiophene analogue of naphthofuran 3mer **10** also showed an alternating mountain-valley fold conformation.[28] These results can be explained by considering that the warped naphthalene ring along its long axis is slightly more stable than the twisted naphthalene ring and/or the conformation cancels the effect of the dipole moments for each distorted naphthalene ring, which is preferred. The energy barrier of inversion for naphthofuran 2mer **6** is estimated to be about 1.7 kcal/mol by DFT calculations at the B3LYP/6-31G(d,p) level. This value is smaller than that of the rotation barrier of ethane (2.88 kcal/mol). Therefore, the conformation of the oligonaphthofurans is not fixed in the alternating mountain-valley shape, but rather the respective naphthalene rings can easily flip-flop within the oligonaphthofuran molecules.

Optical Properties of Oligonaphthofurans. With the series of oligonaphthofurans (2mer **6**, 3mer **10**, 4mer **14**, 6mer **22**, and 8mer **25**) in hand, we then studied their optical properties. Figure 4 shows the UV−vis spectra of the oligonaphthofurans.

As the number of naphthalene rings increased from 2mer **6** to 4mer **14**, consistent red and hyperchromic shifts were observed. Thus, the spectrum maintained its shape and shifted to a longer wavelength with a deeper absorption intensity. However, for 6mer **22** and 8mer **25**, although consistent red shifts were observed, the spectral shape deviated from the original form. These observations indicated that the HOMO−LUMO energy gaps were constantly decreasing. On the other hand, the molar absorption coefficients (ε) that represent the

dx.doi.org/10.1021/ja502209w | J. Am. Chem. Soc. 2014, 136, 7101−7109

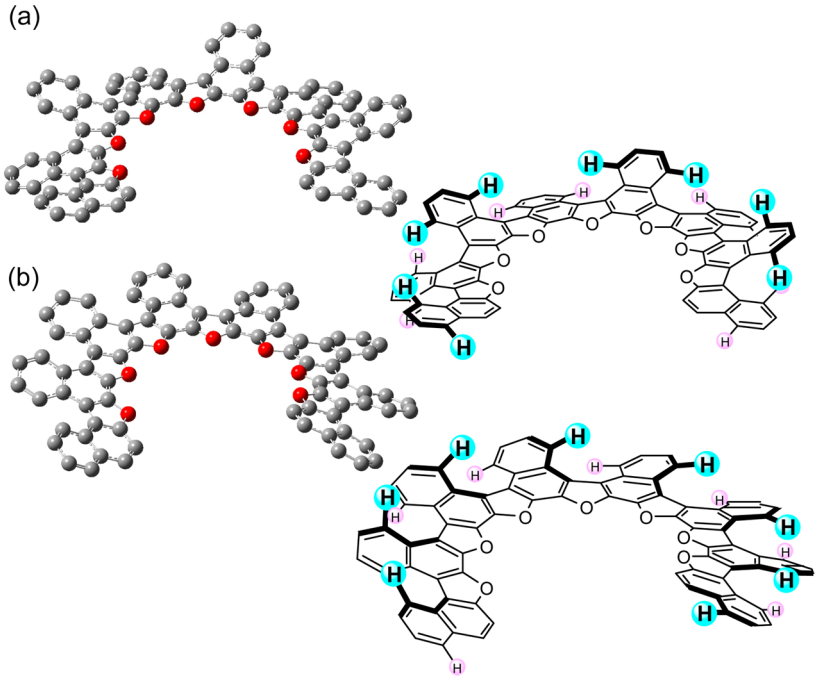

Figure 3. Two optimized conformational structures of the naphthofuran 8mer. Optimized structures were obtained by DFT calculations at the B3LYP/6-31G(d,p) level for the (a) alternating mountain-valley folds conformation and (b) the homochiral screw-shaped conformation. The nonyl side chain was replaced by hydrogen for the DFT calculations.

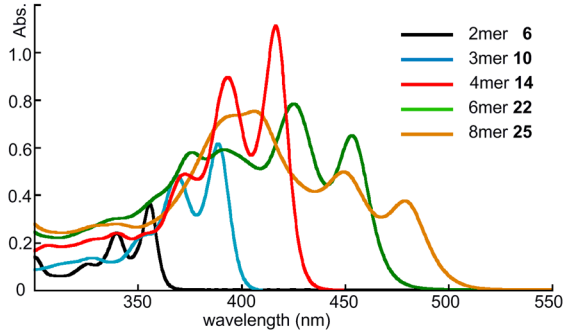

Figure 4. UV–vis spectra of the oligonaphthofurans **6**, **10**, **14**, **22**, and **25**. Conditions: CH_2Cl_2, 20 °C, concentration = 1.0×10^{-5} M, light path length = 1 cm.

probabilities of the corresponding HOMO–LUMO transitions were gradually suppressed as the number of aromatic rings in the oligonaphthofurans increased.

Figure 5 shows an estimation of the HOMO and LUMO by DFT at the B3LYP/6-31G(d,p) level for the naphthofurans 4mer, 6mer and 8mer. These calculations provided the following information. (1) Both the HOMO and LUMO were spread throughout the entire molecule. (2) The orbital coefficients of the HOMO and LUMO increased from the edge to the center of the molecule, which is likely a major factor for the convex curve. (3) With respect to one naphthalene unit, larger coefficients were observed for the inner benzene ring. Therefore, the π-conjugates on the molecule mainly came from the furan rings and the inner benzene rings. (4) Furthermore, the conjugates of the double bonds of the inner benzene rings and the furan rings appeared to be similar to polyacetylenes linked in a *s-cis* fashion (relevant *s-cis* bonds shown in red in Figure 5). These HOMO and LUMO properties, especially property 2, are reasons for the observed constant red shifts in absorption and the decrease in ε of the fan-shaped oligonaphthofurans.

It is important to compare the properties of these compounds to discuss other types of oligoaromatic compounds. Figure 6 shows the maximum absorption in the long wavelength region (λ_{max}) as a function of the number of aromatic rings in oligoaromatic compounds for (a) oligonaphthofurans, (b) oligonaphthalenes **5**,[15f,29] (c) acenes **1**,[2] (d) rylenes **3**,[1d] (e) oligofurans **4**,[14] and (f) ethene-bridged *p*-phenylenes **2**.[3]

For oligonaphthalenes **5** (Figure 6b), a negligible red shift in λ_{max} was observed because of the orthogonal arrangement of the neighboring naphthalene rings. In contrast, the planar acenes **1** and the rylenes **3** have sharp linear relationships because of the effective spread of the π resonance system over the entire molecule (Figure 6c and d). The correlation curves for the oligonaphthofurans, oligofuran **4**, and ethene-bridged *p*-phenylene **2** are convex in shape (Figure 6a, e, and d). These data indicate that the extension of the π resonance system depends on the shape of the aromatic systems, the direction of extension of the aromatic rings, and the conjugation of the π fragments.

Furthermore, Figure 7 shows plots of the transition energies (eV) of the oligoaromatic compounds and the reciprocal of the number of aromatic rings (n).[30] For each oligoaromatic compound, a clear linear correlation exists between λ_{max} and $1/n$. The slope of each linear approximation reflects the pitch of the decrease in the HOMO–LUMO energy gaps for the aromatic rings. Thus, the slope shows the efficiency of π conjugation for each oligoaromatic compound. The linear approximation equations for the oligoaromatic compounds are as follows: (a) oligonaphthofurans, $E = 2.41 + 5.66/n$ ($R = 0.986$); (b) oligonaphthalenes, $E = 3.98 + 1.11/n$ ($R = 0.983$); (c) acenes, $E = 0.52 + 7.02/n$ ($R = 0.998$); (d) rylenes, $E = 1.02 + 5.82/n$ ($R = 0.983$); (e) oligofurans, $E = 2.42 + 3.95/n$ ($R =$

dx.doi.org/10.1021/ja502209w | J. Am. Chem. Soc. 2014, 136, 7101–7109

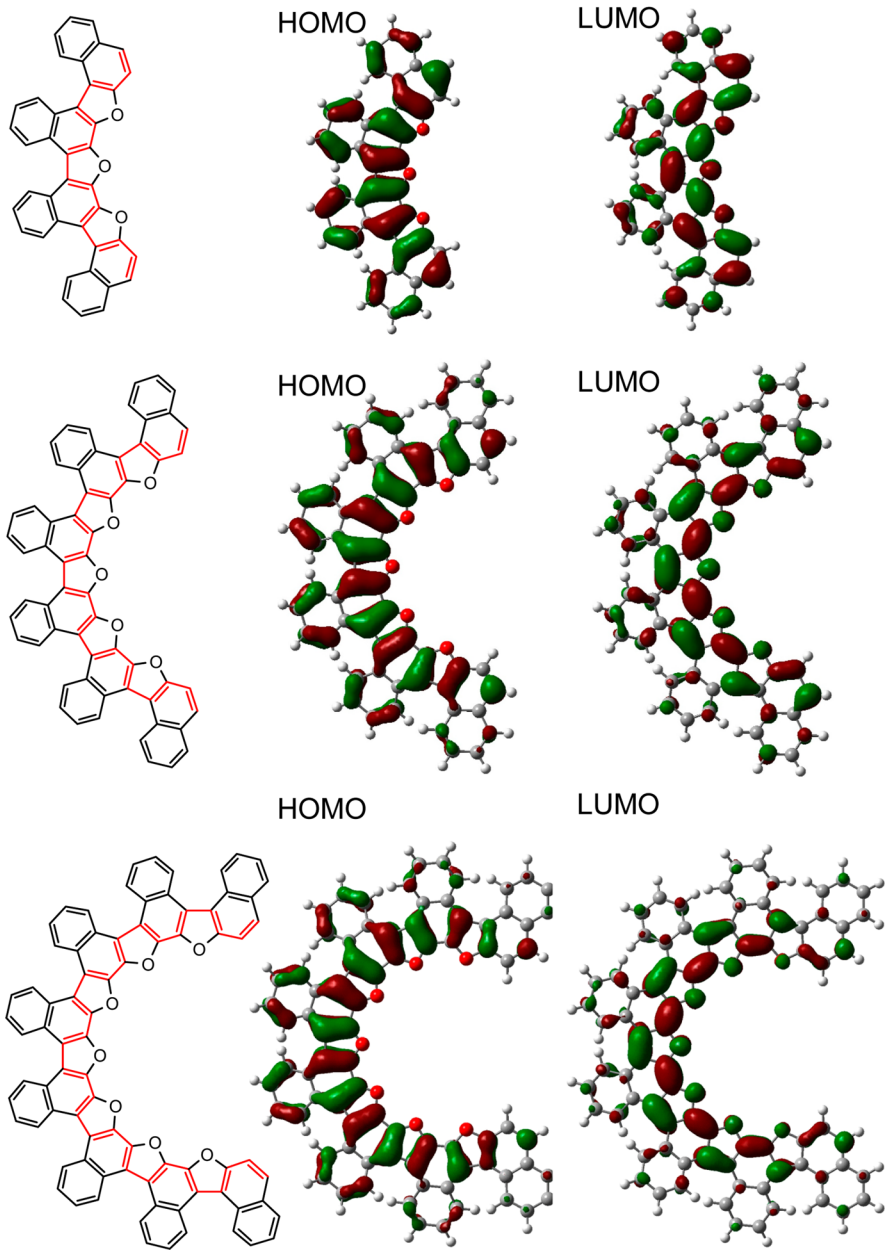

Figure 5. Optimized structures of the naphthofuran 4mer, 6mer, and 8mer with their HOMOs and LUMOs. DFT calculations were at the B3LYP/6-31G(d,p) level, with the nonyl side chain replaced by hydrogen.

0.999); (f) ethene-bridged *p*-phenylenes, $E = 2.63 + 2.28/n$ ($R = 0.997$). It is logical that rigid and planar acenes (c) and rylenes (d) have large slopes (7.02 and 5.82, respectively), whereas the orthogonal oligonaphthalene has a small slope (1.11). The slope of the oligonaphthofuran (5.66) is comparable to those of acenes and rylenes and is clearly larger than that of the oligofuran (3.95) and the ethene-bridged *p*-phenylene (2.28). Despite their fan shape (not linear) and their 3D (not planar) and dynamic (not rigid) π-system, oligonaphthofurans show an effective spreading of the π resonance system.

Figure 8 and Table 1 summarize the standardized fluorescence spectra of the oligonaphthofurans and their characteristic parameters, respectively. Each oligonaphthofuran shows a high quantum yield with a small Stokes shift.

Aggregation Behavior of the Oligonaphthofurans. For higher-order oligonaphthofurans, especially 8mer **25**, aggregation behavior was observed. Figure 9a–c shows the variable-concentration UV–vis spectra of 2mer **6**, 6mer **22**, and 8mer **25** in $CHCl_3$. When the concentration of 2mer **6** was changed from 2×10^{-5} to 1×10^{-6} M, its molar absorption coefficient (ε) remained the same (Figure 9a). In contrast, the corresponding extinction coefficients of 6mer **22** and 8mer **25** obviously decreased as the concentration increased (Figure 9b and c). Furthermore, in the variable-temperature UV–vis spectra of 8mer **25** (Figure 10), as the temperature was lowered from 60 to 20 °C, the UV–vis spectrum of 8mer **25** gradually red-shifted and several isosbestic points were present (expanded in Figure 10b–d). This spectral behavior is attributed to the formation of aggregates at higher concentrations or at lower temperatures.

Figure 11a and b shows the variable-temperature fluorescence spectra of 6mer **22** and 8mer **25**. With an increase in temperature the intensity of the emission of 6mer **22** decreased,

dx.doi.org/10.1021/ja502209w | *J. Am. Chem. Soc.* 2014, 136, 7101–7109

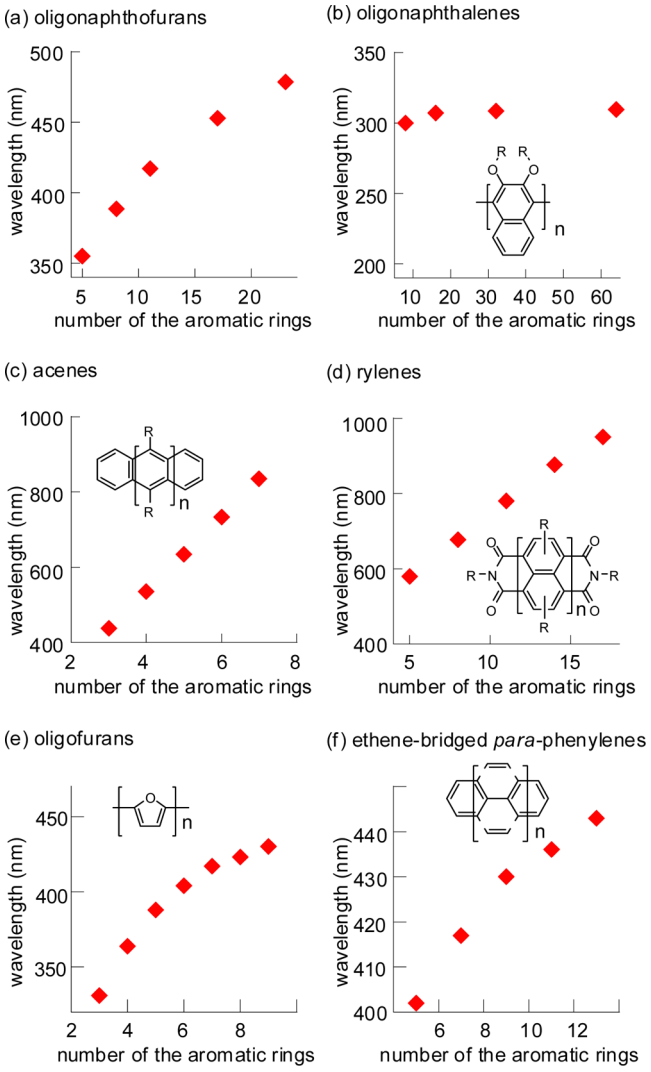

Figure 6. Correlation between λ_{max} and the number of the aromatic rings in oligoaromatic compounds. The plotted data are taken from (b) refs 15f and 29, (c) ref 2, (d) ref 1d, (e) ref 14, and (f) ref 3. For the precise chemical structures of these oligoaromatic compounds see the Supporting Information.

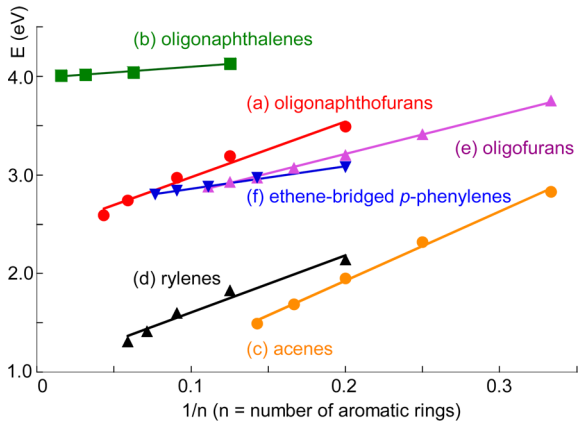

Figure 7. Linear correlations between λ_{max} and $1/n$ for the oligoaromatic compounds.

whereas that of 8mer **25** increased. With an increase in temperature the thermal relaxation process took precedence

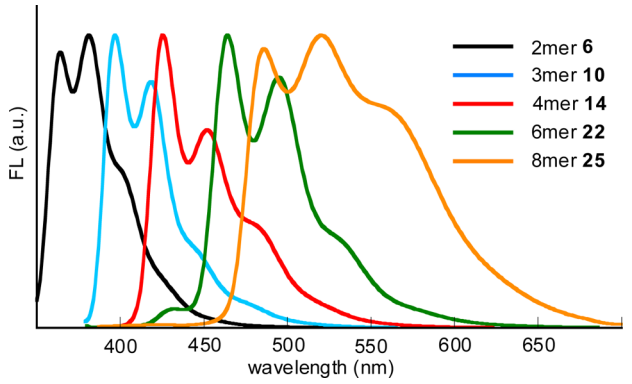

Figure 8. Fluorescence spectra of the oligonaphthofurans **6**, **10**, **14**, **22**, and **25**. Conditions: CH_2Cl_2, 20 °C, concentration = 5.0×10^{-7} M, light path length = 1 cm. λ_{ex} = 340 nm for **6**, 370 nm for **10**, and 380 nm for **14**, **22**, and **25**.

Table 1. Optical Properties of the Oligonaphthofurans

naphthofuran	$\lambda_{abs,max}$ (nm)	λ_{em} (nm)	Stokes shift (nm)	Φ (%)[a]
6	355.5	364	8.5	47
10	389	397	8.5	74
14	417	429	12	69
22	453	464	11	76
25	478.5	486	7.5	50

[a]Fluorescence quantum yields were determined using a solution of quinine sulfate in 1 N H_2SO_4 as a reference standard (Φ = 0.546).

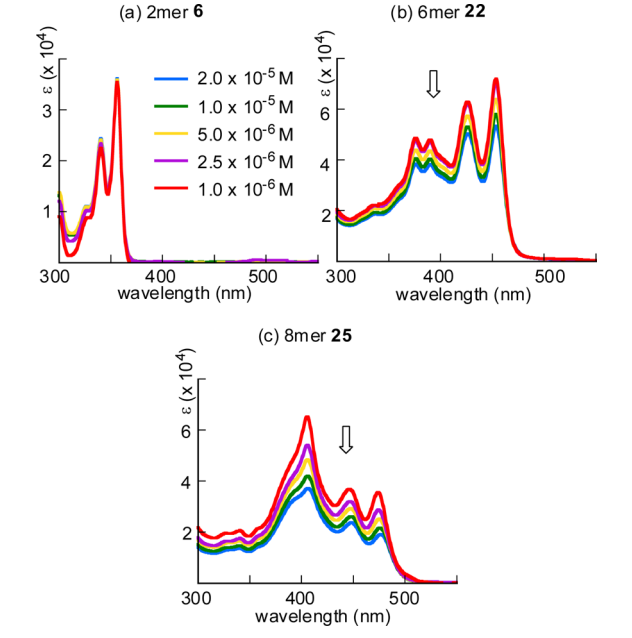

Figure 9. Variable-concentration UV−vis spectra of 2mer **6**, 6mer **22**, and 8mer **25**. Conditions: $CHCl_3$, 20 °C, light path length = 1 cm.

over the fluorescence process for 6mer **22**, while dissociation from the aggregate of 8mer **25** enhanced the fluorescence from the monomer or the lower-order aggregate.

CONCLUSION

We synthesized fan-shaped oligonaphthofurans (up to an 8mer) by repeating a bottom-up method. As the number of units increased, the construction of the furan ring by dehydration became more difficult. The formation of a central

dx.doi.org/10.1021/ja502209w | J. Am. Chem. Soc. 2014, 136, 7101−7109

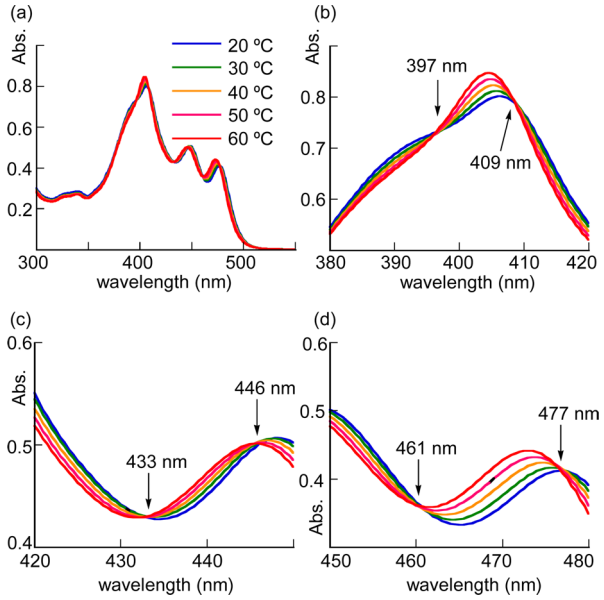

Figure 10. Variable-temperature UV−vis spectra of 8mer **25**. Conditions: $CHCl_3$, concentration = 1.0×10^{-5} M, light path length = 1 cm. Panels b−d show enlargements of panel a to clarify the isosbestic points.

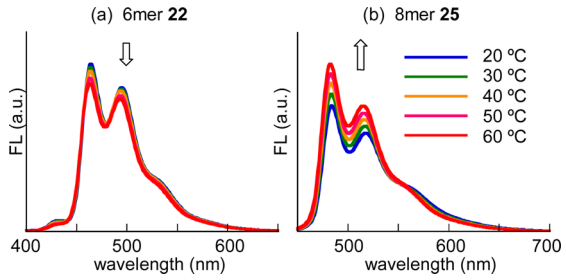

Figure 11. Variable-temperature fluorescence spectra of 6mer **22** and 8mer **25**. Conditions: $CHCl_3$, 5.0×10^{-7} M, light path length = 1.0 cm.

furan during the final stage was especially troublesome because of an abrupt increase in the distortion strain. To avoid this problem, we developed a continuous furan ring formation route via a (2+2+2+2)-8mer to achieve the desired fan-shaped naphthofuran 8mer in 16% yield at 160 °C for 1 month.

An evaluation of the optical properties of these oligonaphthofurans revealed that as the number of aromatic rings increased (1) the λ_{max} of the UV−vis spectrum steadily shifted to longer wavelengths, and (2) the shapes of the UV−vis spectra became deformed compared with the original form. Although the 3D π-resonance system was unevenly spread over the fan-shaped oligonaphthofurans, even as the number of aromatic rings increased, the HOMO−LUMO coefficients were distributed in a gradual manner over the central part of the fan-shaped molecules. The oligonaphthofurans showed an effective spreading of the π resonance system as well as rigid acenes and rylenes. Furthermore, calculations showed the potency of the *s-cis* fixed polyacetylene property on the oligonaphthofuran skeletons. We believe that these properties provide extremely useful basic knowledge for the development of new features in 3D π-systems. We are currently working on synthesizing macrocyclic oligonaphthofurans.

■ ASSOCIATED CONTENT

Ⓢ Supporting Information

Experimental procedures and ^1H and ^{13}C NMR spectra for all new compounds, the coordinates of oligonaphthofurans used in the DFT calculations, and the precise chemical structures of the oligoaromatic compounds in Figure 6. This material is available free of charge via the Internet at http://pubs.acs.org.

■ AUTHOR INFORMATION

Corresponding Author

tsubaki@kpu.ac.jp

Notes

The authors declare no competing financial interest.

■ ACKNOWLEDGMENTS

The authors are grateful to Prof. Yasujiro Murata, Prof. Atsushi Wakamiya, and Prof. Michihisa Murata (ICR, Kyoto University) for their useful suggestions and discussions. We also want to thank Ms. Akiko Fujihashi (ICR, Kyoto University) for the mass spectral analyses and Ms. Kyoko Ohmine (ICR, Kyoto University) for the NMR measurements. This work was supported in part by the Collaborative Research Program of Institute for Chemical Research, Kyoto University (nos. 2012-60 and 2013-48), the Iketani Science and Technology Foundation (no. 0221002-A), and the Sumitomo Foundation (no. 100010).

■ REFERENCES

(1) For recent reviews: (a) Watson, M. D.; Fechtenkötter, A.; Müllen, K. *Chem. Rev.* **2001**, *101*, 1267−1300. (b) Pascal, R. A., Jr. *Chem. Rev.* **2006**, *106*, 4809−4819. (c) Wu, J.; Pisula, W.; Müllen, K. *Chem. Rev.* **2007**, *107*, 718−747. (d) Weil, T.; Vosch, T.; Hofkens, J.; Peneva, K.; Müllen, K. *Angew. Chem., Int. Ed.* **2010**, *49*, 9068−9093. (e) Sun, Z.; Wu, J. *Aust. J. Chem.* **2011**, *64*, 519−528.

(2) (a) Payne, M. M.; Parkin, S. R.; Anthony, J. E. *J. Am. Chem. Soc.* **2005**, *127*, 8028−8029. (b) Purushothaman, B.; Bruzek, M.; Parkin, S. R.; Miller, A.-F.; Anthony, J. E. *Angew. Chem., Int. Ed.* **2011**, *50*, 7013−7017. (c) Anthony, J. E. *Angew. Chem., Int. Ed.* **2008**, *47*, 452−483.

(3) Chen, T.-A.; Lee, T.-J.; Lin, M.-Y.; Sohel, S. M. A.; Diau, E. W.-G.; Lush, S.-F.; Liu, R.-S. *Chem.—Eur. J.* **2010**, *16*, 1826−1833.

(4) (a) Pschirer, N. G.; Kohl, C.; Nolde, F.; Qu, J.; Müllen, K. *Angew. Chem., Int. Ed.* **2006**, *45*, 1401−1404. (b) Avlasevich, Y.; Müller, S.; Erk, P.; Müllen, K. *Chem.—Eur. J.* **2007**, *13*, 6555−6561.

(5) Alonso, J. M.; Díaz-Álvarez, A. E.; Criado, A.; Pérez, D.; Peña, D.; Guitián, E. *Angew. Chem., Int. Ed.* **2012**, *51*, 173−177.

(6) Chen, J.-C.; Lee, T.-S.; Lin, C.-H. *Chem.—Eur. J.* **2008**, *14*, 2777−2787.

(7) (a) Shimizu, A.; Tobe, Y. *Angew. Chem., Int. Ed.* **2011**, *50*, 6906−6910. (b) Chase, D. T.; Fix, A. G.; Rose, B. D.; Weber, C. D.; Nobusue, S.; Stochwell, C. E.; Zakharov, L. N.; Lonergan, M. C.; Haley, M. M. *Angew. Chem., Int. Ed.* **2011**, *50*, 11103−11106. (c) Chase, D. T.; Fix, A. G.; Kang, S. J.; Rose, B. D.; Weber, C. D.; Zhong, Y.; Zakharov, L. N.; Lonergan, M. C.; Nuckolls, C.; Haley, M. M. *J. Am. Chem. Soc.* **2012**, *134*, 10349−10352. (d) Shimizu, A.; Kishi, R.; Nakano, M.; Shiomi, D.; Sato, K.; Takui, T.; Hisaki, I.; Miyata, M.; Tobe, Y. *Angew. Chem., Int. Ed.* **2013**, *52*, 6076−6079. (e) Miyoshi, H.; Nobusue, S.; Shimizu, A.; Hisaki, I.; Miyata, M.; Tobe, Y. *Chem. Sci.* **2014**, *5*, 163−168.

(8) For reviews: (a) Tsefrikas, V. M.; Scott, L. T. *Chem. Rev.* **2006**, *106*, 4868−4884. (b) Wu, Y.-T.; Siegel, J. S. *Chem. Rev.* **2006**, *106*, 4843−4867.

(9) (a) Sakurai, H.; Daiko, T.; Hirao, T. *Science* **2003**, *301*, 1878. (b) Amaya, T.; Hirao, T. *Chem. Commun.* **2011**, *47*, 10524−10535.

(10) (a) Omachi, H.; Segawa, Y.; Itami, K. *Acc. Chem. Res.* **2012**, *45*, 1378−1389. (b) Sisto, T. J.; Jasti, R. *Synlett* **2012**, *23*, 483−489.

(c) Hirst, E. S.; Jasti, R. *J. Org. Chem.* **2012**, *77*, 10473−10478. (d) Sisto, T. J.; Golder, M. R.; Hirst, E. S.; Jasti, R. *J. Am. Chem. Soc.* **2011**, *133*, 15800−15802. (e) Yamago, S.; Watanabe, Y.; Iwamoto, T. *Angew. Chem., Int. Ed.* **2010**, *49*, 757−759. (f) Hitosugi, S.; Yamasaki, T.; Isobe, H. *J. Am. Chem. Soc.* **2012**, *134*, 12442−12445. (g) Kayahara, E.; Iwamoto, T.; Suzuki, T.; Yamago, S. *Chem. Lett.* **2013**, *42*, 621−623.

(11) (a) Matsui, K.; Segawa, Y.; Namikawa, T.; Kamada, K.; Itami, K. *Chem. Sci.* **2013**, *4*, 84−88. (b) Kayahara, E.; Iwamoto, T.; Takaya, H.; Suzuki, T.; Fujitsuka, M.; Majima, T.; Yasuda, N.; Matsuyama, N.; Seki, S.; Yamago, S. *Nat. Commun.* **2013**, *4*, 2694.

(12) A heptagon-embedded hexabenzocoronene was also reported as a curved polycyclic aromatic molecule; see: Luo, J.; Xu, X.; Mao, R.; Miao, Q. *J. Am. Chem. Soc.* **2012**, *134*, 13796−13803.

(13) Izumi, T.; Kobashi, S.; Takimiya, K.; Aso, Y.; Otsubo, T. *J. Am. Chem. Soc.* **2003**, *125*, 5286−5287.

(14) Gidron, O.; Diskin-Posner, Y.; Bendikov, M. *J. Am. Chem. Soc.* **2010**, *132*, 2148−2150.

(15) (a) Tsubaki, K. *Org. Biomol. Chem.* **2007**, *5*, 2179−2188. (b) Takaishi, K.; Tsubaki, K.; Tanaka, H.; Miura, M.; Kawabata, T. *Yakugaku Zasshi* **2006**, *126*, 779−787. (c) Tsubaki, K.; Miura, M.; Morikawa, H.; Tanaka, H.; Kawabata, T.; Furuta, T.; Tanaka, K.; Fuji, K. *J. Am. Chem. Soc.* **2003**, *125*, 16200−16201. (d) Tsubaki, K.; Tanaka, H.; Takaishi, K.; Miura, M.; Morikawa, H.; Furuta, T.; Tanaka, K.; Fuji, K.; Sasamori, T.; Tokitoh, N.; Kawabata, T. *J. Org. Chem.* **2006**, *71*, 6579−6587. (e) Tsubaki, K.; Takaishi, K.; Sue, D.; Kawabata, T. *J. Org. Chem.* **2007**, *72*, 4238−4241. (f) Sue, D.; Takaishi, K.; Harada, T.; Kuroda, R.; Kawabata, T.; Tsubaki, K. *J. Org. Chem.* **2009**, *74*, 3940−3943.

(16) For selected references on oligonaphthalenes, see: (a) Pu, L. *Chem. Rev.* **1998**, *98*, 2405−2494. (b) Guo, W.; Faggi, E.; Sebastián, R. M.; Vallribera, A.; Pleixats, R.; Shafir, A. *J. Org. Chem.* **2013**, *78*, 8169−8175. (c) Marin, G. H.; Horak, V. *J. Org. Chem.* **1994**, *59*, 4267−4271. (d) Bělohradský, M.; Buděšínský, M.; Günterová, J.; Hodačová, J.; Holý, P.; Závada, J.; Císařová, I.; Podlaha, J. *Tetrahedron* **1996**, *33*, 11013−11024.

(17) (a) Tsubaki, K.; Takaishi, K.; Sue, D.; Matsuda, K.; Kanemitsu, Y.; Kawabata, T. *J. Org. Chem.* **2008**, *73*, 4279−4282. (b) Tsubaki, K.; Takaishi, K.; Tanaka, H.; Miura, M.; Kawabata, T. *Org. Lett.* **2006**, *8*, 2587−2590.

(18) Takaishi, K.; Kawamoto, M.; Tsubaki, K. *Org. Lett.* **2010**, *12*, 1832−1835.

(19) Recently, butterfly-shaped expanded naphthofurans were reported. Nakanishi, K.; Sasamori, T.; Kuramochi, K.; Tokitoh, N.; Kawabata, T.; Tsubaki, K. *J. Org. Chem.* **2014**, *79*, 2625−2631.

(20) Additionally, furan ring and/or furan containing conjugated π systems have been receiving much attention as organic electronic materials. See: (a) Bunz, U. H. F. *Angew. Chem., Int. Ed.* **2010**, *49*, 5037−5040. (b) Brown, R. C. D. *Angew. Chem., Int. Ed.* **2005**, *44*, 850−852. (c) Tsuji, H.; Mitsui, C.; Ilies, L.; Sato, Y.; Nakamura, E. *J. Am. Chem. Soc.* **2007**, *129*, 11902−11903. (d) Nakano, M.; Niimi, K.; Miyazaki, E.; Osaka, I.; Takimiya, K. *J. Org. Chem.* **2012**, *77*, 8099−8111. (e) Nakahara, K.; Mitsui, C.; Okamoto, T.; Yamagishi, M.; Miwa, K.; Sato, H.; Yamano, A.; Uemura, T.; Takeya, J. *Chem. Lett.* **2013**, *42*, 654−656. (f) Mitsui, C.; Okamoto, T.; Matsui, H.; Yamagishi, M.; Matsushita, T.; Soeda, J.; Miwa, K.; Sato, H.; Yamano, A.; Uemura, T.; Takeya, J. *Chem. Mater.* **2013**, *25*, 3952−3956.

(21) (a) Aratani, N.; Takagi, A.; Yanagawa, Y.; Matsumoto, T.; Kawai, T.; Yoon, Z. S.; Kim, D.; Osuka, A. *Chem.—Eur. J.* **2005**, *11*, 3389−3404. (b) Aratani, N.; Osuka, A.; Kim, Y. H.; Jeong, D. H.; Kim, D. *Angew. Chem., Int. Ed.* **2000**, *39*, 1458−1462.

(22) (a) Tsuda, A.; Osuka, A. *Science* **2001**, *293*, 79−82. (b) Kim, D.; Osuka, A. *Acc. Chem. Res.* **2004**, *37*, 735−745. (c) Ikeda, T.; Aratani, N.; Osuka, A. *Chem.—Asian J.* **2009**, *4*, 1248−1256.

(23) (a) Areephong, J.; Ruangsupapichart, N.; Thongpanchang, T. *Tetrahedron Lett.* **2004**, *45*, 3067−3070. (b) Xie, X.; Zhang, T. Y.; Zhang, Z. *J. Org. Chem.* **2006**, *71*, 6522−6529.

(24) (a) Danjo, H.; Hirata, K.; Noda, M.; Uchiyama, S.; Fukui, K.; Kawahata, M.; Azumaya, I.; Yamaguchi, K.; Miyazawa, T. *J. Am. Chem. Soc.* **2010**, *132*, 15556−15558. (b) Sato, Y.; Yamasaki, R.; Saito, S. *Angew. Chem., Int. Ed.* **2009**, *48*, 504−507. (c) Makino, T.; Yamasaki, R.; Saito, S. *Synthesis* **2008**, *6*, 859−864. (d) Ooi, T.; Kameda, M.; Maruoka, K. *J. Am. Chem. Soc.* **2003**, *125*, 5139−5151.

(25) Cu/amine promoted oxidative coupling reactions, see: (a) Brussee, J.; Jansen, A. C. A. *Tetrahedron Lett.* **1983**, *24*, 3261−3262. (b) Brussee, J.; Groenendijk, J. L. G.; te Koppele, J. M.; Jansen, A. C. A. *Tetrahedron* **1985**, *41*, 3313−3319. (c) Smrčina, M.; Lorenc, M.; Hanuš, V.; Sedmera, P.; Kočovský, P. *J. Org. Chem.* **1992**, *57*, 1917−1920. (d) Smrčina, M.; Poláková, J.; Vyskočil, Š.; Kočovský, P. *J. Org. Chem.* **1993**, *58*, 4534−4538. (e) Habaue, S.; Seko, T.; Okamoto, Y. *Macromolecules* **2003**, *36*, 2604−2608. (f) Nakajima, M.; Miyoshi, I.; Kanayama, K.; Hashimoto, S.; Noji, M.; Koga, K. *J. Org. Chem.* **1999**, *64*, 2264−2271. (g) Li, X.; Yang, J.; Kozlowski, M. C. *Org. Lett.* **2001**, *3*, 1137−1140. (h) Li, X.; Hewgley, J. B.; Mulrooney, C. A.; Yang, J.; Kozlowski, M. C. *J. Org. Chem.* **2003**, *68*, 5500−5511. (i) Xie, X.; Phuan, P.-W.; Kozlowski, M. C. *Angew. Chem., Int. Ed.* **2003**, *42*, 2168−2170. (j) Mulrooney, C. A.; Li, X.; DiVirgilio, E. S.; Kozlowski, M. C. *J. Am. Chem. Soc.* **2003**, *125*, 6856−6857.

(26) The oxidative coupling was quite sensitive toward some amines; isopropylamine (10% yield), phenylethylamine (~5% yield), diisopropylamine (72% yield).

(27) Frisch, M. J.; Trucks, G. W.; Schlegel, H. B.; Scuseria, G. E.; Robb, M. A.; Cheeseman, J. R.; Scalmani, G.; Barone, V.; Mennucci, B.; Petersson, G. A.; Nakatsuji, H.; Caricato, M.; Li, X.; Hratchian, H. P.; Izmaylov, A. F.; Bloino, J.; Zheng, G.; Sonnenberg, J. L.; Hada, M.; Ehara, M.; Toyota, K.; Fukuda, R.; Hasegawa, J.; Ishida, M.; Nakajima, T.; Honda, Y.; Kitao, O.; Nakai, H.; Vreven, T.; Montgomery, Jr., J. A.; Peralta, J. E.; Ogliaro, F.; Bearpark, M.; Heyd, J. J.; Brothers, E.; Kudin, K. N.; Staroverov, V. N.; Kobayashi, R.; Normand, J.; Raghavachari, K.; Rendell, A.; Burant, J. C.; Iyengar, S. S.; Tomasi, J.; Cossi, M.; Rega, N.; Millam, J. M.; Klene, M.; Knox, J. E.; Cross, J. B.; Bakken, V.; Adamo, C.; Jaramillo, J.; Gomperts, R.; Stratmann, R. E.; Yazyev, O.; Austin, A. J.; Cammi, R.; Pomelli, C.; Ochterski, J. W.; Martin, R. L.; Morokuma, K.; Zakrzewski, V. G.; Voth, G. A.; Salvador, P.; Dannenberg, J. J.; Dapprich, S.; Daniels, A. D.; Farkas, O.; Foresman, J. B.; Ortiz, J. V.; Cioslowski, J.; Fox, D. J. *Gaussian 09*, Revision C.01; Gaussian, Inc.: Wallingford, CT, 2009.

(28) Sadorn, K.; Sinananwanich, W.; Areephong, J.; Nerungsi, C.; Wongma, C.; Pakawatchai, C.; Thongpanchang, T. *Tetrahedron Lett.* **2008**, *49*, 4519−4521.

(29) Taken from the doctoral thesis of Dr. D. Fukatsu (Kyoto University, http://hdl.handle.net/2433/142490). The values are 300.0 nm (for the all-(*S*)-naphthalene 4mer), 307.0 nm (for the all-(*S*)-naphthalene 8mer), 308.5 nm (for the all-(*S*)-naphthalene 16mer), and 309.5 nm (for the all-(*S*)-naphthalene 32mer), respectively.

(30) (a) Bidan, G.; De Nicola, A.; Enée, V.; Guillerez, S. *Chem. Mater.* **1998**, *10*, 1052−1058. (b) Meier, H.; Stalmach, U.; Kolshorn, H. *Acta Polym.* **1997**, *48*, 379−384.